

# Occurrence of small colloids in sea water

Mark L. Wells & Edward D. Goldberg

Scripps Institution of Oceanography, La Jolla, California 92093-0220, USA

COLLOIDAL particles in sea water may be important in the marine chemistry of elements such as carbon and iron<sup>1,2</sup>. Non-living, submicrometre particles (0.4–1.0  $\mu\text{m}$ ) have recently been found to be abundant ( $10^6$ – $10^7$  particles  $\text{ml}^{-1}$ ) in the north Pacific<sup>3</sup> and off Nova Scotia<sup>4</sup>, but smaller colloidal particles in sea water remain largely uncharacterized. Here we report that marine colloids <120 nm in size are at least three orders of magnitude more abundant than larger submicrometre particles. Moreover, the distribution with depth of these small colloids differs markedly from that reported for their larger counterparts<sup>3</sup>. This vertical stratification suggests that small colloidal particles in sea water are reactive. Examination by transmission electron microscopy and energy-dispersive X-ray spectroscopy indicates that the colloids are largely organic, although trace metals (Fe, Al, Co) may also be present. The existence of such colloids may contribute to the discrepancy between standard and new high-temperature methods for measuring dissolved organic carbon<sup>1</sup>.

Seawater samples were collected in Santa Monica Basin 15 km from shore (33°45.07' N, 118°55.09' W, 908 m depth) during June and September 1990. Samples were obtained with modified Niskin bottles (silicone-rubber coated springs), transferred to acid-cleaned 250-ml Teflon bottles and preserved with  $\text{HgCl}_2$  (added to give 1  $\mu\text{M}$  Hg). The samples were wrapped with foil to exclude light and refrigerated for periods up to 1 week before analysis.

Colloids were collected directly on specimen grids for transmission electron microscopy (TEM) by ultracentrifugation, in a modification of the method of Nomizu and Mizuike<sup>5</sup>. Microscope fields ranging in magnification from 42,000 $\times$  to 52,000 $\times$  were selected from different specimen grid openings

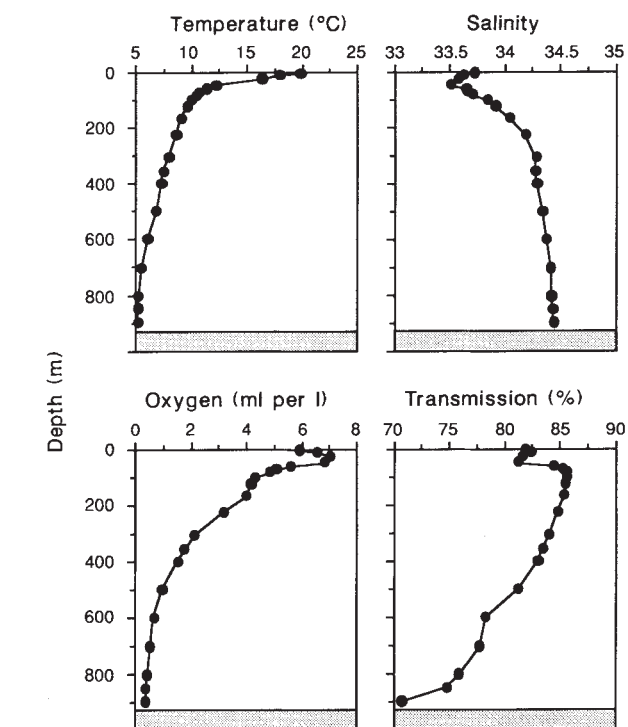


FIG. 2 Physical data for station 305 in Santa Monica basin in July 1990. Comparable data were not available for the September cruise.

and photographed. Colloid numbers and size distributions were then determined by computer image analysis of the digitized TEM micrographs. Elemental compositions of some colloids were determined qualitatively by energy-dispersive X-ray spectroscopy (EDS).

Vertical profiles taken in July and September showed that colloids <120 nm in size were highly stratified. Concentrations remained below detection limits ( $\leq 10^4$  particles  $\text{ml}^{-1}$ ) at the surface, increased sharply near the lower thermocline (40–100 m) to  $>10^9$  particles  $\text{ml}^{-1}$ , and decreased again to  $<10^4$  particles  $\text{ml}^{-1}$  below the thermocline (Fig. 1). This distribution is substantially different from that reported for larger (0.4–1.0  $\mu\text{m}$ ) colloids in the northwest Pacific, where surface con-

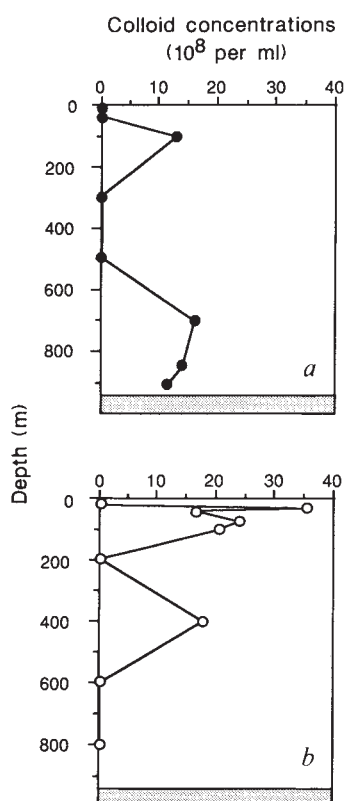


FIG. 1 Vertical profiles of the number of small colloids (5–120 nm) at station 305 in Santa Monica basin (33°45.10' N, 118°55.09' W) on a, 9 July and b, 1 September 1990. Seawater samples (10 ml) were centrifuged (Beckman L7) in a swing bucket rotor (SW41) at 288,000  $g$  for 4.0 h at 25 °C. Settling colloids were collected on 200-mesh copper TEM specimen grids placed in specially constructed holders at the bottom of 13-ml polyallomer centrifuge tubes (Beckman). The grids, coated with carbon-stabilized formvar (Ted Pella®), were first rendered hydrophilic by 60 s of glow discharge under vacuum<sup>12</sup>. After centrifugation, the supernatant was removed slowly and the grids rinsed gently with five sequential tube volumes of filtered (0.1  $\mu\text{m}$  Nuclepore) distilled water. The air-dried grids were examined in a Phillips CM 30 transmission electron microscope at 100 kV. Between 200 and 500 colloids were counted in each field, and five to eight fields were photographed from each sample. The detection limit for colloid numbers was constrained by the field area at 42,000 $\times$ , the lowest magnification at which 5–10 nm colloids were still visible; two to three colloids per field corresponded to a detection limit of  $\sim 1 \times 10^4$  colloids  $\text{ml}^{-1}$ . Final particle concentrations were calculated taking into account the taper correction for nonparallel particle trajectories during centrifugation<sup>13</sup>. Colloid recovery efficiencies were obtained by adding known amounts of colloidal haematite ( $\sim 600$  nm in size) and latex microspheres (88 nm) to sea water; these were  $97 \pm 13\%$  and  $93 \pm 0.2\%$ , respectively. The precision for colloid enumeration was  $<10\%$  ( $\pm 1$  s.d.). Samples and specimen grids were handled under 'clean' conditions in a laminar flow airbench (Class 100); few, if any, colloids were observed in analytical blanks processed in the same way as the samples.

centrations decreased sharply with depth<sup>3</sup>. The distribution of colloids in deep waters differed markedly between July and September. In July, colloid concentrations in bottom waters (700–910 m) were  $>10^9$  particles  $\text{ml}^{-1}$ , and thus similar to those near the thermocline. By contrast, deep-water concentrations in September were high at 400 m ( $1.5 \times 10^9$  particles  $\text{ml}^{-1}$ ) but remained below the detection limit in bottom waters (Fig. 1*b*). The vertical distribution of small colloids in July did not co-vary with temperature, salinity, dissolved oxygen or light transmission (Fig. 2).

The extreme vertical variation in colloid abundance with depth is surprising, yet we submit that this finding is valid. First, the precision for estimating colloid concentrations on individual specimen grids is better than  $\pm 10\%$  (1 s.d. for  $n \geq 6$ ), and triplicate samples taken from the same Niskin bottles yield numbers within this precision. The addition of  $\text{HgCl}_2$  does not alter the colloid abundance or size distribution even after five days of storage<sup>2</sup>, longer than the delay between collection and processing for most samples in this study. Successive 4-h centrifugations yielded colloids only after the initial spin. Gentle prefiltering ( $<155$  nm Hg,  $0.4 \mu\text{m}$  Nuclepore) of raw sea water before centrifugation did not significantly alter the numbers or size distribution of small colloids recovered (not shown), indicating that they were not artefacts arising from the breakup of larger particles during centrifugation. Vertical distributions of colloids at other stations 30 km and 150 km off the California coast show

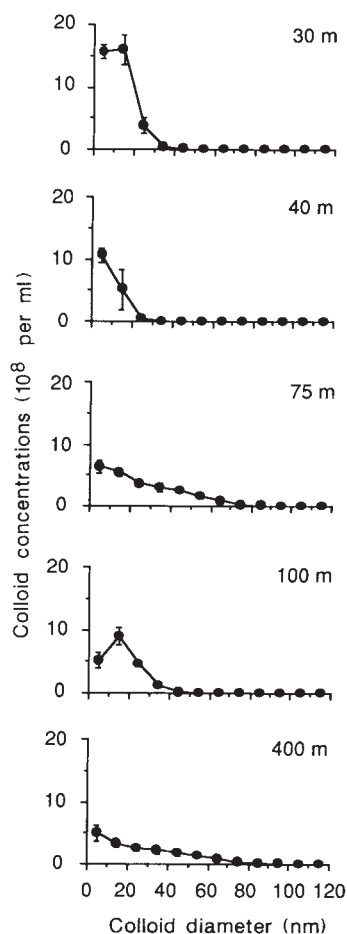


FIG. 3 The size distribution of small colloids collected from five depths at station 305, Santa Monica basin, September 1990. Colloid diameter was taken as twice the minor axis of a theoretical ellipse having the same two-dimensional area as the colloid; size spectra determined this way were not significantly different from those of ruler measurements of the narrowest dimension of colloids in the micrographs. It should be noted that colloid dimensions may have been altered by settling on the formvar film or by dehydration.

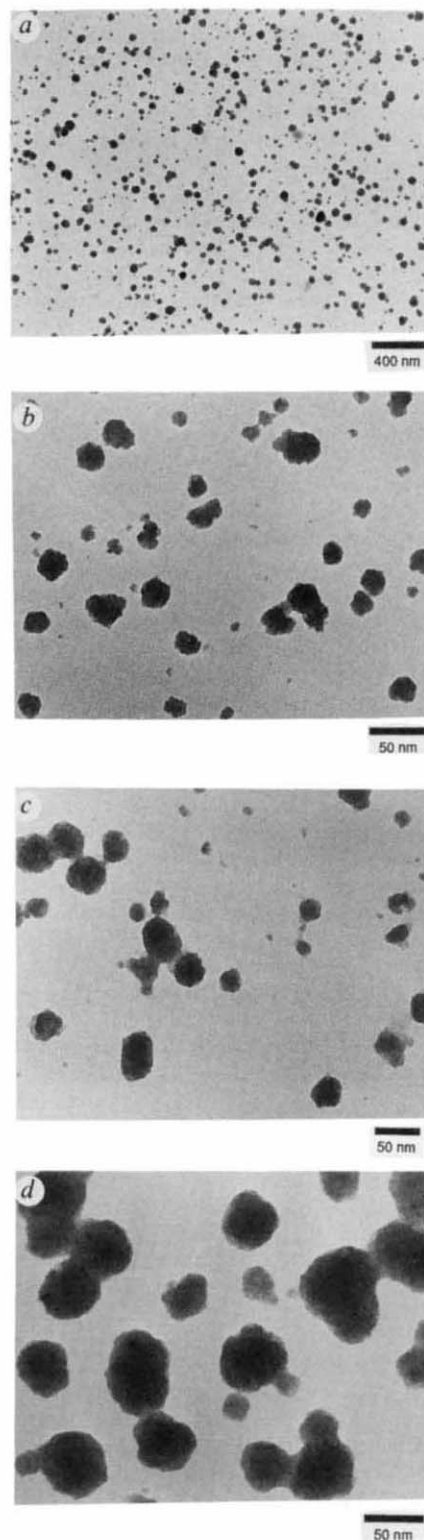


FIG. 4 Transmission electron micrographs from samples collected at station 305, Santa Monica basin in September 1990. The spatial distribution of colloids on the membranes tended to be uniform, as shown for the 75-m sample (*a*). Enlarged views of the colloids from 75 m and 400 m depth are shown in *b* and *c*, respectively. Most of the colloids were globular and rounded, and had low electron opacity, suggesting an organic composition (contrast in these micrographs was enhanced during development). Many appeared to be aggregates of smaller granules 2–10 nm in size, some of which were darker in contrast indicating an inhomogeneous colloid composition. *d*, A similar inhomogeneous, aggregative morphology is seen clearly in colloids from 850 m in July 1990.

common features, with high abundances in the region of the thermocline and numbers below detection in deeper waters (M.L.W. and E.D.G., manuscript in preparation). Colloids were also abundant in surface (1 m) sea water 2 km offshore of the Scripps Institution of Oceanography from February through April<sup>2</sup> when upwelling conditions predominated. Colloid numbers fell below the detection limit, however, in July and August when upwelling ceased and the water column became stratified (as were conditions in Santa Monica basin during the time of sampling). It should be noted that values reported here as  $<10^4$  particles  $\text{ml}^{-1}$  do not indicate that colloids of  $<0.1 \mu\text{m}$  are completely absent, but that their small numbers prevented quantification.

The size spectrum below 120 nm diameter showed an increase in colloid numbers with decreasing size that was nearly logarithmic in some cases (Fig. 3). This size relationship may be considerably more pronounced than indicated here because the smallest size classes ( $<40 \text{ nm}$ ) may not have been collected in representative numbers by 4 h of centrifugation. Logarithmic size distributions are very common for marine particles  $>1.0 \mu\text{m}$  (ref. 6) and these findings indicate that this general relationship extends into the smallest of the colloidal phases.

The nature and composition of these small colloids can be inferred from high-resolution TEM images and EDS analyses. The  $<120 \text{ nm}$  size class included marine viruses and, less frequently, inorganic crystalline materials. But by far the most abundant components of this size class are discrete, relatively diffuse colloids having low electron opacity (Fig. 4a-d). The colloids tended to be rounded in shape and many appeared to be aggregates of smaller granules  $\sim 2\text{--}10 \text{ nm}$  in size. Microfibrils, such as those found abundantly in fresh-water lakes<sup>7,8</sup>, were not found. The low electron opacity of these colloids suggests that they are largely organic, although dark (high-contrast) granules were often observed within them, indicating an inhomogeneous composition (Fig. 4b-d). The colloid morphology was similar in shallow and deep waters, perhaps indicating a common source or mechanism of their formation.

In appearance, these colloids bear a striking resemblance to transmission electron micrographs of soil-derived fulvic acids, which also show a granular, aggregated morphology<sup>9,10</sup>. A granule size of 2–5 nm corresponds to  $\sim 10,000$  daltons<sup>9,11</sup>, which is well within the range for dissolved organic carbon (DOC) fractions measured in sea water<sup>1</sup>. EDS analysis of colloids from surface and deep waters yielded rather patternless spectra, which is consistent with a largely organic matrix. Most of the colloids examined fell below the instrumental size limit suggested for 'quantitative' EDS analyses ( $\sim 100 \text{ nm}$ ). All of the particles examined, however, were slightly enriched in Fe, Co, Si, Al and O (19 particles examined). In some cases, Cr, Ca, Ni and V were also detected.

The vertical stratification (and therefore nonconservative behaviour) of these small colloids, coupled with their apparent organic nature, suggest they are derived primarily from biological processes and that they have short residence times in sea water (although the colloid suspensions seem to be stable<sup>2</sup> for at least five days in refrigerated sea water preserved with  $\text{HgCl}_2$ ). It is not clear what processes produce the depth distributions found. The occurrence of these colloids in waters off the Scripps Institution of Oceanography<sup>2</sup> and on the outer continental slope off Point Conception, California (M.L.W. and E.D.G., manuscript in preparation) indicates that they are dispersed widely in marine waters. If their composition is typical of biological debris, they could account for up to  $\sim 10\%$  of DOC in these waters (assuming spherical shape, a mean density of  $1.1 \text{ g cm}^{-3}$ , 50% C by weight and  $1.0 \text{ mg l}^{-1}$  DOC), and may contribute to the discrepancy between standard and new high-temperature methods for DOC determinations<sup>1</sup>. Furthermore, the apparent close association of metals with these colloids suggests that they may play an important part in the transport and fate of trace elements in sea water. □

Received 7 February; accepted 29 July 1991.

1. Sugimura, Y. & Suzuki, Y. *Mar. Chem.* **24**, 105–131 (1988).
2. Wells, M. L. & Goldberg, E. D. *Mar. Chem.* (in the press).
3. Koike, I., Hara, S., Terauchi, K. & Kogure, K. *Nature* **345**, 242–244 (1990).
4. Longhurst, A. *et al. Deep-Sea Res.* (submitted).
5. Nomizu, T. & Mizuike, A. *A. Mikrochim. Acta* **1**, 65–72 (1986).
6. McCave, I. N. *Deep-Sea Res.* **31**, 329–352 (1984).
7. Leppard, G. G., Massalski, A. & Lean, D. R. S. *Protoplasma* **92**, 289–309 (1977).
8. Leppard, G. G. *Arch. Hydrobiol.* **101**, 521–530 (1984); *Water Res.* **20**, 697–702 (1986).
9. Leppard, G. G., Buffle, J. & Baudat, R. *Water Res.* **20**, 185–196 (1986).
10. Schnitzer, M. & Kodama, H. *Geoderma* **13**, 279–287 (1975).
11. Williams, P. M. in *Plankton Dynamics of the Southern California Bight* (ed. Eppley, D.) 53–83 (Springer, New York, 1986).
12. Hayat, M. A. *Basic Techniques for Transmission Electron Microscopy* 234–235 (Academic, Orlando, 1986).
13. Mathews, J. & Buthala, D. A. *J. Virology* **5**, 598–603 (1970).

ACKNOWLEDGEMENTS. We thank G. Hemingway, E. Ringer, and W. Cochlan for collecting water samples on our behalf. We also thank P. Buseck and W. Su for assistance with EDS measurements. This study was funded by ONR.

## Structural transformation of quartz at high pressures

N. Binggeli & James R. Chelikowsky

Department of Chemical Engineering and Materials Science and Minnesota Supercomputer Institute, University of Minnesota, Minneapolis, Minnesota 55455, USA

THE behaviour of  $\alpha$ -quartz, one of the most common tetrahedrally coordinated silica polymorphs, at high pressures has been the subject of several experimental studies. At room temperature, gradual pressure-induced amorphization is observed (at about 25–35 GPa)<sup>1,2</sup>, followed at higher pressures (above 60 GPa) by a transformation to a crystalline octahedrally coordinated 'rutile-like' structure<sup>3</sup>. The driving force for these transformations is not well understood. We report here first-principles calculations of the electronic and structural properties of the high-pressure structure of  $\alpha$ -quartz, which show a pressure-induced transformation of the oxygen sublattice to a body-centred cubic structure. The main features of cubic packing are present at 30 GPa, and the ideal form is achieved at about 60 GPa. The formation of the cubic sublattice facilitates structural transformations involving a change in Si coordination. In the oxygen body-centred cubic lattice, a small displacement of Si ions along the empty channels of the structure is sufficient to transform  $\alpha$ -quartz either to a structure with mixed fourfold/sixfold coordination or, for a larger silicon displacement, to a purely sixfold-coordinated structure. This description is consistent with the evidence of intermediate crystalline phases with mixed Si coordination above the amorphization pressure in molecular-dynamics simulations<sup>4</sup>, and can also explain the transformation to a sixfold crystalline structure at higher pressure.

Silica, an important constituent of the Earth's crust, exists in a number of allotropic forms. Among the various silica polymorphs,  $\alpha$ -quartz is the stable structure at room temperature and at pressure below 3 GPa. At higher pressures, this structure persists as a metastable phase which gradually transforms to an amorphous state and then to a crystalline structure in which Si is sixfold coordinated. The nature of the amorphous state is not known. Molecular-dynamics simulations based on a two-body potential by Tsuneyuki *et al.*<sup>4</sup> suggest that this phase may contain sixfold and fourfold coordinated Si atoms. In some of these simulations, the authors found that quartz transforms to crystalline phases with mixed fourfold/sixfold coordinations above 30 GPa. In other simulations, they found a transformation to a sixfold coordinated phase above 30 GPa, and they propose that in high-pressure experiments compression of a macroscopic sample would produce coexistence of domains of the different phases.

The model of polyhedral tilting<sup>5</sup> generally used to describe the structural changes in silica polymorphs consisting of corner-